

**JAST (Journal of Animal Science and Technology) TITLE PAGE**  
**Upload this completed form to website with submission**

ARTICLE INFORMATION	Fill in information in each box below
<b>Article Type</b>	Research article
<b>Article Title (within 20 words without abbreviations)</b>	Functional characteristics of a pig 2D intestinal organoid model as an in vitro platform for nutritional studies
<b>Running Title (within 10 words)</b>	Characteristics of pig organoid models for nutritional research
<b>Author</b>	Sang Seok Joo <sup>1</sup> , Bon-Hee Gu <sup>2</sup> , Eunbyeol Lee <sup>1</sup> , Eunseon Oh <sup>3</sup> , Minji Kim <sup>4</sup> , Hyunjung Jung <sup>4</sup> , Myunghoo Kim <sup>1,5,*</sup>
<b>Affiliation</b>	1 Department of Animal Science, College of Natural Resources & Life Science, Pusan National University, Miryang 50463, Korea 2 Life and Industry Convergence Research Institute, Pusan National University, Miryang 50463, Korea 3 Application Center, CJ Blossom Park, Suwon 16495, Korea 4 Animal Nutrition and Physiology Division, National Institute of Animal Science, Rural Development Administration, Wanju 55365, Korea 5 Institute for Future Earth, Pusan National University, Busan 46241, Korea
<b>ORCID (for more information, please visit <a href="https://orcid.org">https://orcid.org</a>)</b>	Sang Seok Joo ( <a href="https://orcid.org/0000-0001-8909-1102">https://orcid.org/0000-0001-8909-1102</a> ) Bon-Hee Gu ( <a href="https://orcid.org/0000-0001-7368-3074">https://orcid.org/0000-0001-7368-3074</a> ) Eunbyeol Lee ( <a href="https://orcid.org/0009-0009-6615-8840">https://orcid.org/0009-0009-6615-8840</a> ) Eunseon Oh ( <a href="https://orcid.org/0009-0007-3766-1805">https://orcid.org/0009-0007-3766-1805</a> ) Minji Kim ( <a href="https://orcid.org/0000-0003-2106-1921">https://orcid.org/0000-0003-2106-1921</a> ) Hyunjung Jung ( <a href="https://orcid.org/0000-0002-7004-2017">https://orcid.org/0000-0002-7004-2017</a> ) Myunghoo Kim ( <a href="https://orcid.org/0000-0002-8444-6952">https://orcid.org/0000-0002-8444-6952</a> )
<b>Competing interests</b>	No potential conflict of interest relevant to this article was reported.
<b>Funding sources</b> State funding sources (grants, funding sources, equipment, and supplies). Include name and number of grant if available.	This research was supported by Basic Science Research Program through the National Research Foundation of Korea (NRF) funded by the Ministry of Education (No. 2022R1A6A3A13063610) and Learning & Academic research institution for Master's PhD students and Postdocs (LAMP) Program of the National Research Foundation of Korea (NRF) grant funded by the Ministry of Education (No. RS-2023-00301938).
<b>Acknowledgements</b>	The authors thank technical and financial supports from all members of the Application Center at the CJ Blossom Park (Suwon, Republic of Korea)
<b>Availability of data and material</b>	Upon reasonable request, the datasets of this study can be available from the corresponding author.
<b>Authors' contributions</b> Please specify the authors' role using this form.	Conceptualization: Joo SS, Kim M (Myunghoo Kim). Data curation: Joo SS, Gu BH. Formal analysis: Joo SS, Gu BH, Lee E. Methodology: Joo SS, Gu BH, Kim M (Minji Kim). Software: Oh E, Kim M (Minji Kim). Validation: Jung HJ, Kim M (Myunghoo Kim) Investigation: Joo SS, Lee E, Oh E. Writing - original draft: Joo SS, Lee E, Kim M (Myunghoo Kim). Writing - review & editing: Joo SS, Gu BH, Lee E, Oh E, Kim M (Minji Kim), Jung HJ, Kim M (Myunghoo Kim).
<b>Ethics approval and consent to participate</b>	The experimental protocols describing the management and care of animals were reviewed and approved by the Animal Care and Use Committee of Chungbuk National University, Cheongju, Korea (approval#CBNUA-1421-20-02).

**CORRESPONDING AUTHOR CONTACT INFORMATION**

<b>For the corresponding author (responsible for correspondence, proofreading, and reprints)</b>	<b>Fill in information in each box below</b>
First name, middle initial, last name	Myunghoo Kim
Email address – this is where your proofs will be sent	mhkim18@pusan.ac.kr
Secondary Email address	
Address	Department of Animal Science, College of Natural Resources & Life Science, Pusan National University, Miryang 50463, Korea
Cell phone number	+82-10-3082-3598
Office phone number	+82-55-350-5803
Fax number	+82-55-350-5519

ACCEPTED

1 **Abstract**

2 Intestinal epithelial cell lines have been widely used in the field of biomedical and livestock research, and recently,  
3 the use of organoid systems has been attempted. However, they have several limitations as an in vitro platform in  
4 particularly in nutrition-related studies. Thus, this study aimed to compare the existing in vitro platform (IPEC-J2 cell  
5 line) with a three-dimension (3D) organoid model, and to understand the nutritional phenomena occurring in the  
6 intestinal lumen through the establishment and characterization of a two-dimension (2D) organoid model. By  
7 comparing the IPEC-J2 cell line and 3D intestinal organoids, we found differences in intestinal epithelial cell types,  
8 including nutrient-related enteroendocrine cells and enterocytes. 3D organoids have most of gut epithelial cell types,  
9 but IPEC-J2 did not. We further established a 2D organoid model with an exposed apical membrane and compared it  
10 with a 3D organoid model. The established 2D organoids had higher expression of enteroendocrine cells and  
11 enterocyte marker genes, and most genes were related to nutritional properties (nutrient transporters, hormones, and  
12 digestive enzymes). Fatty acids, one of the nutrients, were added to the two organoid models for comparison.  
13 Fluorescence image analysis confirmed that more fatty acids were absorbed by 2D organoids. Treatment with a long-  
14 chain fatty acid mixture increased the expression of fatty acid receptor (*FFAR1* and *FFAR4*) and hormone (*GCG*,  
15 *CCK*, and *PYY*) genes in 2D organoids but not in 3D organoids, leading to the activation of metabolic responses. The  
16 more facilitated metabolic process was observed in 2D organoids by increased mitochondria activity and ATP  
17 production. Our findings emphasize that pig intestinal organoid systems, particularly 2D organoid model, is better in  
18 vitro platform, particularly in nutrition-related studies. Compared with other in vitro platforms, 2D organoids can be  
19 used for studying intestinal epithelial cell-nutrient interactions structurally and characteristically. Our study provides  
20 a basis for utilizing a pig 2D intestinal organoid model as a potentially advanced in vitro system for intestinal epithelial  
21 cell-based nutritional research in domestic animals.

22

23 **Keywords:** Pig organoids, 2D organoid model, Nutrition, Enteroendocrine cells, Enterocytes

24

25

## Introduction

26

27 Pigs are one of the major livestock, with pork accounting for more than a quarter of the total protein consumed  
28 worldwide and approximately 35% of the total meat production [1]. Pigs are recognized as important livestock, and  
29 various studies are being conducted to increase their productivity. The health status of pigs is influenced by a  
30 combination of multiple factors, including genetics, environmental stress, pathogen infection, and nutrition [2-4].  
31 Among these factors, nutrition is particularly related to gut health, and numerous studies have focused on enhancing  
32 gut health in pigs. For example, positive indicators related to gut health, such as reduced diarrhea incidence, increased  
33 tight junction protein gene expression, and improved intestinal morphology, were identified when plant-derived oils  
34 rich in n-3 polyunsaturated fatty acids were fed to weaned piglets as feed additive [5]. In contrast, an in vitro study  
35 using the pig intestinal epithelial cell line, IPEC-J2, examined the effects of functional nutrients on gut health. For  
36 example, acetate and propionate enhance cell viability and gut barrier integrity [6].

37 Recently, because of animal welfare issues, methods that can replace animal experiments have attracted  
38 considerable attention. However, in vitro studies in domestic animals are limited. Organoid culture systems can  
39 mimic and reproduce tissue functions and properties. For example, organoid systems are highly similar to living  
40 organisms and can be applied in genetic engineering, making them economically and efficiently suitable for high-  
41 throughput screening [7]. In addition, organoids have the characteristics of cell populations related to organs, which  
42 enables the study of interactions with factors related to these organs. A representative example is the intestinal  
43 organoid-based co-culture system used in mechanistic studies [8]. In a study by Hou et al., an organoid-based co-  
44 culture model with lamina propria immune cells isolated from the intestine was developed, and the immune cell-  
45 epithelium regulatory mechanism of *Lactobacillus reuteri*, a well-known probiotic, was investigated. Thus,  
46 organoid-based co-culture models are recognized as advanced tools with the potential for in vitro research on  
47 biological processes [9, 10]. Intestinal organoids can be generated using embryonic, pluripotent, and adult stem  
48 cells [11]. These stem cells can be cultured under appropriate culture medium conditions without a specific feeder  
49 cell [12]. For example, isolated crypts, which contain adult stem cells, undergo self-renewal, organization,  
50 morphogenesis, and differentiation within the crypt-villus structure [13]. Crypt-derived intestinal organoids exhibit  
51 structural and functional similarities to the gut.

52 Recently, various intestinal organoids have been developed for livestock, including cattle, sheep, chicken, and  
53 pigs [14-17]. Many studies have investigated intestinal diseases induced by pathogenic microbes and viruses in pig  
54 gut organoids. Disease-inducing microbes such as *Salmonella typhimurium* and *Toxoplasma gondii* can directly

55 infect pig organoids [18]. In a study by Li et al., a transmissible gastroenteritis virus, a pig enteric coronavirus, was  
56 found to infect pig jejunal organoids. In a previous study, apical-out and two-dimension (2D) culture methods were  
57 used due to structural limitations in three-dimension (3D) culture, which is the basic organoid culture method [19].  
58 Pathogens mainly infect the intestinal lumen, and most nutrient uptake and sensing occurs in the intestinal lumen,  
59 resulting in metabolic processes. Thus, the 2D organoid model has several advantages as an in vitro research platform  
60 because it can simulate phenomena occurring in the intestinal lumen.

61 Although studies on pig intestinal organoids have been actively conducted, the characteristics of these platforms  
62 remain unclear. Therefore, this study aimed to compare the characteristics of the existing pig intestine in vitro platform  
63 with pig organoids, and to establish a 2D organoid model for better intestinal epithelial cell research. A 2D organoid  
64 model was developed to simulate external exposure of the lumen using pig 3D organoids, and the physiological and  
65 nutritional characteristics were compared. Our results suggest the possibility of using the 2D pig organoid model in  
66 nutritional research.

67

68

## Materials and Methods

### 69 Cell culture

70 IPEC-J2, a pig intestinal cell line, was kindly provided by Prof. Yun of Seoul National University. IPEC-J2 cells were  
71 cultured in a 90 mm cell culture dish (SPL Life Sciences, Pocheon, Korea) using DMEM/F12 medium (Thermo Fisher  
72 Scientific, Waltham, MA, USA), supplemented with 10% fetal bovine serum, 100 U/mL penicillin, and 100 µg/mL  
73 streptomycin (Thermo Fisher Scientific) at 37 °C in a humidified 5% CO<sub>2</sub> atmosphere. For RNA extraction and  
74 immunofluorescence staining,  $5 \times 10^5$  cells were seeded to 6-well plates (SPL Life Sciences) and 35 mm confocal  
75 dishes (SPL Life Sciences) for 2 days.

76 R-spondin 1 and Wnt-3a are critical factors in pig intestinal organoids. To procure them, two cell lines expressing  
77 the target proteins were used in cell culture-conditioned media. Conditioned media were prepared as described  
78 previously [20]. Briefly, R-spondin 1-expressing HEK293T cells and L Wnt-3A cells (CRL-2647™, ATCC, Manassas,  
79 VA, USA) were cultured in a 90 mm cell culture dish using DMEM medium (Thermo Fisher Scientific), supplemented  
80 with 10% fetal bovine serum, 100 U/mL penicillin, and 100 µg/mL streptomycin, with selective antibiotics for 2-3  
81 passages. The selective antibiotics used were: 0.2 mg/mL Hygromycin B (Thermo Fisher Scientific) for HEK 293T  
82 cells and 0.4 mg/mL G-418 (Thermo Fisher Scientific) for L Wnt-3A cells. To obtain a high concentration of  
83 conditioned media, the cells were initially cultured ( $5 \times 10^5$  cells in a 90 mm cell culture dish) for 7 days using

84 advanced DMEM/F12 medium (Thermo Fisher Scientific) with 10% fetal bovine serum, 100 U/mL penicillin, and  
85 100 µg/mL streptomycin. Briefly, cells were grown for 4 days (approximately 8-90% confluence at this point) in  
86 harvest media (first batch). The medium was replaced with fresh culture medium, and the cells were cultured for  
87 another 3 days in the harvest media (second batch). Finally, the first and second batches were mixed and filtered in a  
88 1:1 ratio and stored at -20 °C until further use.

89

### 90 **Isolation of pig small intestinal crypts for organoid culture**

91 In this study, three jejunal fragments were harvested from 3-week-old weaned piglets, all of which were healthy and  
92 asymptomatic. For crypt isolation, 3-4 cm of the gut tissue was harvested and opened longitudinally. To remove  
93 luminal contents and mucus, they were gently scraped using slide glass and vigorously washed with phosphate-  
94 buffered saline (PBS, Thermo Fisher Scientific). The gut tissues were then cut to 0.5 × 0.5 cm<sup>2</sup> pieces and transferred  
95 to a crypt isolation solution containing 30 mM ethylene-diamine-tetra acetic acid (EDTA, Thermo Fisher Scientific)  
96 and 1 mM DL-dithiothreitol (DTT, Sigma-Aldrich, St. Louis, MO, USA). The tissue fragments were incubated for 30  
97 min on ice in a horizontal shaking incubator at 100 rpm. After incubation, the tissue fragments were transferred to a  
98 cold crypt washing buffer containing 54.9 mM D-sorbitol (Sigma-Aldrich) and 43.4 mM sucrose (Sigma-Aldrich) in  
99 PBS, and gently shaken for 2 min to release the crypts. To obtain pure crypts, the supernatant was transferred to a new  
100 tube using 100 µm cell strainer (SPL Life Sciences) and centrifuged at 200 × g for 5 min. The crypt pellet was  
101 resuspended in advanced DMEM/F12 medium and counted for pig intestinal organoid culture.

102

### 103 **Culture and maintenance of pig intestinal organoids**

104 The counted pig jejunal crypts were mixed with advanced DMEM/F12 and Matrigel (Corning Inc., Corning, NY,  
105 USA) in a 1:1 ratio. The mixture was seeded into a 96-well cell culture plate (SPL Life Sciences) at a concentration  
106 of 5 crypts/µL (total volume: 4 µL). The plate was then incubated for 30 min in a cell culture incubator to solidify the  
107 Matrigel mixture. Next, 100 µL of pig intestinal organoid culture medium was added to each well, and medium  
108 composition was as follows: advanced DMEM/F12 supplemented with 1x N2 supplement (Thermo Fisher Scientific),  
109 1x B27 supplement (Thermo Fisher Scientific), 2 mM GlutaMAX™ Supplement (Thermo Fisher Scientific), 10 mM  
110 nicotinamide (Sigma-Aldrich), 1 mM N-acetylcysteine (Sigma-Aldrich, St. Louis, MO), 10 mM HEPES (Thermo  
111 Fisher Scientific), 100 µg/mL Primocin™ (InvivoGen, San Diego, CA, USA), 50 ng/mL recombinant murine EGF  
112 (PMG8041, Thermo Fisher Scientific), 100 ng/mL recombinant murine Noggin (250-38, Peprotech, NJ, USA), 10%

113 R-spondin 1 conditioned media, 50% Wnt-3a conditioned media, 10  $\mu$ M SB 202190 (Sigma-Aldrich), 0.5  $\mu$ M A 83-  
114 01 (Sigma-Aldrich), 2.5  $\mu$ M CHIR99021 (Sigma-Aldrich), and 10  $\mu$ M Y-27632 (Selleckchem, Houston, TX, USA).  
115 Pig organoids were cultured for 4 days, and the medium was replaced on day 2. To prevent anoikis in pig organoids,  
116 Y-27632 was added for the first two days only.

117 To maintain pig organoids and develop 2D monolayer organoid, 4-day-cultured organoids were sub-cultured.  
118 Matrigel was dissociated using cell recovery solution (Corning Inc.) at 4 °C for 30 min using an orbital shaker with  
119 slow shaking (60 rpm). The organoid-containing supernatant was collected and centrifuged at  $200 \times g$  for 5 min. Pig  
120 organoid pellets were resuspended in advanced DMEM/F12 and physically pipetted. Organoid fragments were  
121 counted and cultured on a new plate using the methods described above.

122

### 123 **Development of 2D pig intestinal organoids**

124 Sub-cultured organoid fragments were seeded into a 96-well cell culture plate at 12.5 crypts/ $\mu$ L concentration (total  
125 volume: 4  $\mu$ L) and cultured for 2 days. Short-cultured pig organoids were passaged for the sub-culture method, and  
126 organoid pellets were incubated with TrypLE Express Enzyme solution (Thermo Fisher Scientific) with occasional  
127 pipetting for 10 min in a cell culture incubator. Pig organoids dissociated into single cells were centrifuged at  $800$   
128  $\times g$  for 5 min and counted. The single cells were resuspended in 2D pig intestinal organoid culture medium with 20%  
129 (v/v) fetal bovine serum added to the pig intestinal organoid culture medium, and seeded at 150,000 cells/cm<sup>2</sup> in pre-  
130 coated plates. The pre-coating process was carried out by incubating 2% (v/v) Matrigel with advanced DMEM/F12  
131 medium (50  $\mu$ L for 96-well cell culture plate) for 1 h in a cell culture incubator. Before single cell seeding, the coating  
132 solution was removed and the cells were washed once with advanced DMEM/F12.

133

### 134 **Quantitative real-time polymerase chain reaction (qRT-PCR) assay**

135 Total RNA of all samples, including IPEC-J2 cells, 3D organoids, and 2D organoids, was extracted using TRIzol™  
136 Reagent (Thermo Fisher Scientific). The 0.5  $\mu$ g of RNA was used for cDNA synthesis using the AccuPower® RT  
137 PreMix (Bioneer, Daejeon, Korea). qRT-PCR was performed using a QuantStudio 1 Real-Time PCR system (Applied  
138 Biosystems, Waltham, CA, USA) and the following conditions were used: 50 °C for 2 min, 95 °C for 15 min, 95 °C  
139 for 20 s, and 60 °C for 40 s (40 cycles), followed by melting curve analysis. *GAPDH* was used for normalization of  
140 relative gene expression, and the expression level was calculated using the  $2^{-\Delta C_T}$  method [21]. The primer sequences  
141 for the target genes used in this study are presented in Table 1.

142

143 **Imaging and immunofluorescent staining**

144 Inverted and confocal microscopes were used to obtain organoid images. A Nikon Eclipse Ts2R microscope (Nikon,  
145 Tokyo, Japan) was used to obtain day-to-day 3D and 2D organoid images. Immunofluorescent staining was performed  
146 to compare the expression of intestinal epithelial cell markers in IPEC-J2 cells and 3D organoids, and images were  
147 obtained using a confocal microscope. Briefly, the cells were fixed in 2% paraformaldehyde (Biosesang Inc.,  
148 Gyeonggi-do, Korea) for 30 min at room temperature. After washing with PBS, cells were permeabilized with 1%  
149 Triton X-100 (Biosesang Inc.) for 30 min at room temperature. The samples were washed with PBS and blocked with  
150 a blocking buffer (10% goat serum and 0.5% Triton X-100) overnight at room temperature. The primary antibodies  
151 rabbit anti-Muc2 (27675-1-AP, ProteinTech, IL, USA) and mouse anti-ChgA (sc-393941, Sant Cruz Biotechnology,  
152 TX, USA) were diluted at 1:50 and 1:100, respectively, with the blocking buffer. The samples were then incubated  
153 for 4 h at room temperature and washed 5 times using the blocking buffer. After washing step, the secondary antibodies,  
154 goat anti-rabbit IgG Alexa Fluor 488 (A-11034, Thermo Fisher Scientific) for Muc2 and goat anti-mouse Alexa Fluor  
155 488 for ChgA (A-11029, Thermo Fisher Scientific), were diluted at 1:500 using the blocking buffer. The samples were  
156 incubated for 1 h at room temperature in the dark and washed 10 times using the blocking buffer. The samples were  
157 stained with Alexa Fluor 555 phalloidin (Thermo Fisher Scientific) (1:200 diluted in PBS) and Hoechst 33342  
158 (Thermo Fisher Scientific) (1:500 diluted in PBS). Both staining processes were performed sequentially, and the  
159 samples were incubated in the dark for 30 min at room temperature and washed with PBS. After staining, IPEC-J2  
160 cells and 3D organoids were subjected to confocal microscopy (K1-Fluo; Nanoscope Systems, Daejeon, Korea).

161

162 **Fatty acid absorption by pig intestinal organoids**

163 To assay fatty acid uptake, C1-BODIPY-C12 (Thermo Fisher Scientific) was used on 3D and 2D organoids, with  
164 minor modifications [20]. For the 3D organoid assay, Matrigel was solubilized in a cell recovery solution using the  
165 above method. They were resuspended in a solution of 1  $\mu$ M C1-BODIPY-C12 with 10% fatty acid-free bovine serum  
166 albumin solution and incubated in an ultra-low attachment 24-well cell culture plate (Corning Inc., Corning) for 30  
167 min in a cell culture incubator. For the 2D organoid assay, the medium was removed, and they were incubated for 30  
168 min in a cell culture incubator with the same BODIPY solution. The 3D and 2D organoids were fixed in 2%  
169 paraformaldehyde and stained with Hoechst 33342 for image analysis. The intracellular fluorescent signal (fluorescent  
170 size and intensity) was quantified using NIS-Elements Basic Research software (Nikon).



171  
172  
173  
174  
175  
176  
177  
178  
179  
180  
181  
182  
183  
184  
185  
186  
187  
188  
189  
190  
191  
192  
193  
194  
195  
196  
197  
198  
199

### **Lipid mixture (LM) treatment on pig intestinal organoids**

The LM (Sigma-Aldrich) was used to treat both 3D and 2D organoids. It contains non-animal derived fatty acids (2 µg/ml arachidonic acid and 10 µg/ml each linoleic, linolenic, myristic, oleic, palmitic, and stearic acids), 0.22 mg/ml cholesterol from New Zealand sheep's wool, 2.2 mg/ml Tween-80, 70 µg/ml tocopherol acetate, and 100 mg/ml Pluronic F-68 solubilized in cell culture water. Before harvesting the 3D and 2D organoid samples (on day 4 for 3D organoids and on day 2 for 2D organoids), they were treated with 2% LM (v/v) (in each organoid culture medium) for 12-hours. All LM-related organoid experiments, including qRT-PCR, MitoTracker staining, and ADP:ATP ratio assays, were performed using the same method.

### **Mitochondria staining of pig intestinal organoids**

To stain the mitochondria of organoids, MitoTracker™ Green FM (Thermo Fisher Scientific) was used. MitoTracker was prepared as a 1 mM stock in dimethyl sulfoxide according to the manufacturer's instructions. The 3D and 2D organoids were washed once with advanced DMEM/F12, and MitoTracker (final concentration of 100 nM) and Hoechst 33342 (final 1:500 dilution) were added to each organoid culture medium. They were then incubated for 30 min in a cell culture incubator and washed once with advanced DMEM/F12. The stained images were immediately obtained using a confocal microscope.

### **ADP:ATP ratio assay of pig intestinal organoids**

ADP:ATP ratios of 3D and 2D organoids were analyzed according to the bioluminescence method using a SpectraMax iD5 microplate reader (Molecular Devices, San Jose, CA, USA). The assay was conducted using a commercial ADP:ATP Ratio Assay Kit (Abcam, Cambridge, MA, USA) according to the manufacturer's instructions. Briefly, Matrigel was removed from 3D organoids using a cell recovery solution, and single cells were obtained using the TrypLE Express Enzyme solution. After centrifugation, incubation was performed at room temperature for 5 min using the Nucleotide Releasing Buffer of the kit (200 µL per well in a 96-well plate). 2D organoids were washed once with plain advanced DMEM/F12 and incubated at room temperature for 5 min in an equal volume of Nucleotide Releasing Buffer. The remainder of the assay was performed according to the method recommended in the kit using a white 96-well plate (SPL Life Sciences).

## 200 **Statistical analysis**

201 The experimental data from three to five independent experiments were pooled and presented as mean  $\pm$  standard  
202 deviation. For fatty acid absorption assay, five representative organoid images (3D organoids) and five position images  
203 (2D organoids) were randomly selected within each three independent experiments, and fluorescence area and  
204 intensity were measured within selected images (average 4.6 and 9.6 fluorescence signal areas for 3D and 2D  
205 organoids, respectively). To determine whether the data were normally distributed, the Shapiro–Wilk test was  
206 performed using Prism 8 software (GraphPad, La Jolla, CA, USA). Abnormally distributed data were further analyzed  
207 using a two-tailed Mann–Whitney test, and normally distributed data were further analyzed using a two-tailed unpaired  
208 *t*-test. The significant difference between groups was considered at  $p < 0.05$ , and the tendency was considered at  $0.05$   
209  $< p < 0.10$ .

210

211

## **Results**

### 212 **Comparison between the IPEC-J2 cell line and 3D pig organoids**

213 First, the characteristics of the IPEC-J2 cell line, a well-known in vitro pig epithelial cell platform, and pig small  
214 intestinal 3D organoids were compared. To determine the presence of several types of epithelial cells, mRNA  
215 expression levels of epithelial cell marker genes (*LGR5* for crypt-base columnar cells, *LYZ* for Panth cells, *MUC2* for  
216 goblet cells, *CHGA* for enteroendocrine cells, and *ALPI* for enterocytes) were compared. In 3D pig organoids, *LYZ*  
217 and *ALPI* showed significantly higher gene expression than IPEJ-J2 cells. In addition, *MUC2* and *CHGA* were  
218 expressed in 3D pig organoids, but not in the IPEC-J2 cell line (Fig. 1A). *LGR5* was similarly expressed in the  
219 organoids and IPEC-J2 cells. Immunofluorescence staining confirmed the presence of MUC2 and CHGA at the protein  
220 level. MUC2 and CHGA expressions were observed in 3D pig organoids, but not in IPEC-J2 cells (Fig. 1B and C).  
221 These data suggest that pig epithelial cell lines have limitations as in vitro research platforms for studying pig epithelial  
222 cells.

223

### 224 **Comparison of the gene expression of intestinal epithelial cell markers between 3D and 2D pig organoids**

225 Organoids are normally cultured 3D condition, making it difficult to reproduce phenomenon occurring in the intestinal  
226 lumen. As most nutrition-related phenomena occur in the intestinal lumen, a 2D monolayer pig organoid model that  
227 can expose the apical membrane was developed in this study. The 3D organoids were fully grown by day 4 by culturing  
228 approximately 20 sub-cultured organoid fragments. 2D organoids were seeded with approximately 50,000 single cells

229 from sub-cultured 3D organoids and showed more than 90% confluence on day 2 (Fig. 2A). To compare the expression  
230 levels of intestinal epithelial cell marker genes in two fully developed organoids, qRT-PCR was conducted using  
231 epithelial cell marker genes. There were no significant differences in *LGR5*, *LYZ*, and *MUC2* between 3D and 2D  
232 organoids. However, 2D organoids had significantly higher expression of *CHGA* and *ALPI* than 3D organoids (Fig.  
233 2B). Collectively, these results suggest that, in addition to the structural properties of the 2D organoid model, intestinal  
234 epithelial cell marker gene expression differs from that of 3D organoids.

235

### 236 **Comparison of nutritional physiology-related factors in different pig organoid models**

237 Because high expression of *CHGA* and *ALPI*, which are important for nutritional physiological responses, was  
238 observed in the 2D organoid platform, nutritional function-related gene expression was further compared. To  
239 characterize the nutrition-related functions of pig 2D intestinal organoids, the gene expression levels of small intestinal  
240 nutrient transporters, gastrointestinal hormones, and brush border enzymes were compared with those in 3D organoids.  
241 Except for *GLUT5*, a fructose transporter, most nutrient transporters (*SGLT1*: sodium/glucose transporter, *GLUT2*:  
242 glucose transporter, *PEPT1*: peptide transporter, and *CD36*: fatty acid transporter) showed higher gene expression  
243 levels in 2D organoids than in 3D organoids (Fig. 3A). Gastrointestinal hormones are mainly secreted by  
244 enteroendocrine cells and these hormones are classified into families based on structural homology [22, 23]. In this  
245 study, the gastrin family (*GAST* and *CCK*), secretin family (*GCG* and *GIP*), somatostatin family (*SST*), motilin-ghrelin  
246 family (*MLN* and *GHRL*), and PP-fold family (*PYY*) were investigated. Among the various hormone-encoding genes,  
247 *GCG* was not significantly different between 3D and 2D organoids. However, the expression of other hormone-related  
248 genes examined in this study was significantly higher in 2D organoids than in 3D organoids (Fig. 3B). The gene  
249 expression of brush border enzymes secreted by enterocytes was compared between the two types of pig organoids.  
250 The carbohydrate-related (*SI*, *MGAM*, and *LCT*) and peptide-related (*DPEPI* and *ANPEP*) enzyme genes were  
251 significantly highly expressed or tended on 2D organoids than in 3D organoids (Fig. 3C). Collectively, these results  
252 suggest that 2D organoids have higher functional gene expression for nutritional physiological responses.

253

### 254 **Assessment of nutrient absorption in the different types of pig organoid models**

255 To assess nutrient uptake in 3D and 2D pig intestinal organoids, we used fatty acids as one of the nutrients absorbed  
256 by the pig small intestine. To compare the efficiency of fatty acid uptake in each pig organoid model, 3D and 2D  
257 organoids were treated with fluorescent fatty acids (Fig. 4A). On average, more lipid droplets were present in 2D

258 organoid images than in 3D organoids. Consistent with this, a larger fluorescence area and brighter fluorescence  
259 intensity were observed in 2D organoids than in 3D organoids (Fig. 4B). These data suggest that 2D pig organoids  
260 uptake nutrients more efficiently than 3D organoids.

261

### 262 **Changes in the expression of nutrient physiology-related factors in pig organoid models after nutrient exposure**

263 Nutrients are absorbed by intestinal epithelial cells, and nutritional physiological phenomena occur through specific  
264 receptors and binding proteins. To evaluate the influence of nutrients, especially fatty acids, LM containing various  
265 long-chain fatty acids (LCFAs) was treated to 3D and 2D organoids, and selected LCFA-responsive gene expression  
266 was investigated. There was no difference in the gene expression of fatty acid-related receptors (*FFAR1* and *FFAR4*)  
267 and binding proteins (*FABP1*, *FABP2*, and *FABP5*), which are associated with enteroendocrine cells and enterocytes,  
268 in 3D organoids. However, in 2D organoids, a significant increase and increase tendency in the gene expression of  
269 *FFAR1* and *FFAR4* was observed after LM treatment (Fig. 5A and B).

270 Nutrients present in the intestinal lumen or absorbed by enterocytes may act on enteroendocrine cells to regulate  
271 gastrointestinal hormone secretion. Some hormones secreted by the small intestine respond to fatty acids. In this study,  
272 major fatty acid-responsive hormone genes, such as *GCG*, *CCK*, *GIP*, and *PYY* were examined after LM exposure  
273 (Fig. 5C and D). Treatment of 3D organoids with LM showed no difference in hormone genes, but significant increases  
274 in the expression of hormone genes other than *GIP* were observed in 2D organoids. Overall, these results indicate that  
275 the pig 2D organoid model can mimic the nutrient-induced responses occurring in small intestinal epithelial cells, and  
276 that 2D organoids are more responsive to lipid molecules than 3D organoids.

277

### 278 **Nutrient metabolism in pig organoid models**

279 Fatty acids absorbed by intestinal epithelial cells are oxidized by mitochondrial activity to produce energy via ATP  
280 synthesis. To assess fatty acid-induced mitochondrial activity and ATP patterns in organoids, we confirmed the  
281 mitochondria mass and ADP:ATP ratio in LM-treated 3D and 2D organoids. When the two types of organoids were  
282 compared using MitoTracker staining, there was no difference in fluorescence intensity between the control and LM  
283 groups of 3D organoids. However, in 2D organoids, strong fluorescence intensity was observed in the LM group  
284 compared with that in the control group (Fig. 6A). Next, the intracellular ADP:ATP ratios of 3D and 2D pig intestinal  
285 organoids were measured. There was no significant difference between the control and LM groups in 3D organoids.  
286 However, in 2D organoids, the ADP:ATP ratio was significantly reduced by LM treatment (Fig. 6B). These results

287 indicate that the 2D organoid model has a more active metabolic response to fatty acids, such as the conversion of  
288 ADP to ATP, than the 3D organoid model.

289

290

## Discussion

291 The gut is a specialized tissue with multiple functions that interacts with the external environment. The epithelial cell

292 layer of the gut plays an important role in the first physical barrier and immune function against harmful external

293 factors, such as pathogens, viruses, and toxins [24]. The small intestine, a part of the gut, consists of various epithelial

294 cell types. The major cell types include crypt-resident stem cells, Paneth cells, goblet cells, enteroendocrine cells, and

295 enterocytes [25]. Intestinal epithelial cells are continuously regenerated at short intervals, and this phenomenon is due

296 to stem cells differentiating into various cell types through progenitor cells [26]. For regulation of intestinal epithelial

297 cells, the function of intestinal stem cells plays a key role, and the LGR5+ cell in the crypt-base has been considered

298 the sole intestinal stem cell marker, but a recent study has reported that various epithelial cells of the isthmus region

299 beyond the crypt also have a stemness potential and are involved in intestinal epithelial cell homeostasis [27].

300 Therefore, studies related to interactions between multiple cell types are needed to understand the mechanisms of

301 action of complex intestinal epithelial cells. Several cell lines can be used as in vitro platforms to study the responses

302 of intestinal epithelial cells. The inflammatory response regulatory function of short-chain fatty acids, including

303 acetate, propionate, and butyrate, was evaluated in Caco-2 cells, a widely used human intestinal epithelial cell line

304 [28]. Caco-2 cells were treated with 5-Fluorouracil, which is used as a chemotherapy drug for cancer, but caused

305 intestinal mucositis as a side effect, to induce intestinal inflammation. Yue et al. reported that three kinds of short-

306 chain fatty acids inhibit the activation of NLRP3 inflammatory bodies (caspase-1, IL-1 $\beta$ , and IL-18) and increase the

307 expression of gut barrier integrity indicators (Occludin and MUC2) compared with inflammation-induced Caco-2 cells.

308 The use of two human enteroendocrine cell lines, NCL-h716 and HuTu-80, has been reported in studies related to

309 hormone responses, another epithelial cell function [29]. Larraufie et al. reported that short-chain fatty acids

310 (especially propionate and butyrate) strongly regulate hormone production in vitro. The use of epithelial cell lines as

311 an in vitro platform has advantages, such as high reproducibility and economic efficiency. Available epithelial cell

312 lines from domestic animals are very limited thus, the most of domestic animal epithelial cell studies done by using

313 IPEC-J2. For example, probiotic *L. reuteri*, which is isolated from healthy piglet, modulated intestinal health-related

314 factors in LPS-challenged IPEC-J2 cells [30]. Under the challenge conditions, the expression of inflammatory

315 cytokines (TNF- $\alpha$  and IL-6) increased and the expression of tight junction proteins (Claudin-1, Occludin, and ZO-1)

316 expression decreased. However, the above indicators were restored to normal levels through treatment of *L. reuteri*  
317 culture supernatant to IPEC-JC2 cells. However, there are some limitations to using these cell lines in in vitro assays.  
318 For example, because most intestinal epithelial cell lines have only a few epithelial cell types, it is difficult to reproduce  
319 the epithelial cell combination of complex gut tissues. In addition, immortalization is required to make a stable cell  
320 line that can affect the biological function of cell types [31]. Therefore, a better in vitro platform is essential to  
321 understand the function of intestinal epithelial cells, and for this reason, intestinal organoids have recently attracted  
322 attention [32, 33].

323 Intestinal organoids have also been established in domestic animals and their applications have been reported in  
324 various studies, including physiological gut function, immunity, and nutrition [34, 35]. For example, pig organoids  
325 have been used to investigate the mechanism by which deoxynivalenol, a major mycotoxin, inhibits gut epithelial  
326 cell development [36]. Deoxynivalenol does not affect the formation efficiency of organoids, but it reduces the  
327 differentiation efficiency of organoids and proliferation of epithelial cells by suppressing the Wnt/ $\beta$ -catenin  
328 pathway. Domestic animal intestinal organoids can also be used to evaluate immunomodulatory effects of feed  
329 additives. A recent study on the immune response to feed additives containing organic acids and essential oils in *S.*  
330 *enterica* challenged chicken organoid model was reported [37]. Treatment with feed additives reduced the bacterial  
331 load on organoids and downregulated inflammatory responses by decreasing the gene expression of cytokines and  
332 chemokines associated with innate immunity. For intestinal epithelial cell studies, the IPEC-J2 cell line, which is  
333 isolated from the neonatal piglet mid-jejunum and is not transformed, has been used in various research fields and  
334 has provided important insights into dynamic gut physiology [38]. Although the IPEC-J2 cell line is a useful tool  
335 for investigating pig intestines, it has several limitations. For example, unlike other epithelial cell lines, IPEC-J2  
336 cells present a high level of transepithelial resistance, a key parameter of epithelial tightness that affects intracellular  
337 processes [39, 40]. Additionally, a comparison of IPEC-J2 cells and actual pig jejunum tissue under common culture  
338 conditions (using fetal bovine serum) revealed differences in ion transport properties and cell morphology [38].  
339 Recently, a transcriptome analysis of IPEC-J2 cells, jejunal organoid, and primary gut tissue was reported [41]. A  
340 comparison of gene profiling specifically expressed in pig small intestine with primary tissue and in vitro systems  
341 showed a pattern of gene expression similar to that of primary tissue in jejunal organoids rather than IPEC-J2 cells.  
342 In addition, there was a clear difference in epithelial cell type marker gene expression between the gut tissue and  
343 the IPEC-J2 cell line, and the degree of intestinal epithelial cell marker gene expression in primary gut tissue in  
344 organoids was similar. The results of this study suggest that it may be more realistic to use organoid models than

345 cell line-based in vitro platforms to study intestinal epithelial cell regulation in pigs. In our study, *MUC2* (for goblet  
346 cells) and *CHGA* (for enteroendocrine cells) were compared based on gene and protein expression level (by  
347 immunofluorescence), and it was confirmed that they were not expressed in IPEC-J2 cells but expressed in intestinal  
348 organoids. In addition, *LYZ* (for Paneth cells) and *ALPI* (for enterocytes) were highly expressed in pig intestinal  
349 organoids compared with IPEC-J2 cells. Our data suggested that 3D organoids are better in vitro systems as they have  
350 essential epithelial cell types compared with IPEC-J2 cells. In future studies, comparative research on the functions  
351 of epithelial cells should be conducted to determine the advantages of pig intestinal organoids.

352 The intestine has various physiological functions, such as immune regulation, physical barriers to harmful external  
353 materials, and nutrient absorption [25]. Nutrient absorption is mainly mediated by enteroendocrine cells and  
354 enterocytes in intestinal epithelial cells. Enteroendocrine cells and enterocytes are more directly related to nutrition  
355 than other epithelial cell types. Enteroendocrine cells are distributed throughout the epithelium of the gastrointestinal  
356 tract, including the small intestine. They release several gut hormones in response to food intake and control gut  
357 motility or other endocrinal response [42]. Enterocytes are the major cells responsible for nutrient absorption and are  
358 the highest proportion of epithelial cell types [43]. Dietary food delivered to the intestine lumen is broken down into  
359 small units of nutrients by digestive enzymes that are sensed by enteroendocrine cells or enterocytes. Enteroendocrine  
360 cells secrete gastrointestinal hormones that regulate various organ systems, and enterocytes directly absorb small  
361 nutrients [44]. A sequential process involving intestinal digestive enzymes, nutrient-specific transporters, and  
362 hormone secretion is required for this series of nutrient-related processes. The intestinal organoid system has three  
363 characteristic factors and functional response of nutrient use [17, 45]. For example, there was a difference in the degree  
364 of nutrient absorption when nutrient-related transporters were treated with transporter inhibitors or transporter gene  
365 knock-out organoids, and there was also a difference in the levels of secreted hormones in hormone gene knock-out  
366 organoids [45]. These results suggest that the gut organoids play a functional role in nutrient processing. However,  
367 there is no clear information regarding the nutrient process-related functions of 3D organoids compared with those of  
368 IPEC-J2 cells. In our study, we found that 3D organoids differed in the expression of *CHGA* and *ALPI* associated with  
369 the nutrient process compared with the IPEC-J2 cell line (*CHGA*: expressed only in 3D organoids; *ALPI*: higher gene  
370 expression in 3D organoids). Some nutrient process-related gene expression also showed similar differences between  
371 3D organoids and the IPEC-J2 cell line (Fig. S1).

372 Although organoid systems have several advantages, they have structural limitations related to the physical  
373 properties of the intestine. The apical side of epithelial cells, which are in contact with the lumen of the intestine and

374 consist of microvilli, performs various biological functions, such as mucus secretion, gut microbiota sensing, and  
375 nutrient processing [46]. 3D intestinal organoids, a general culture method, are not exposed to the outside of the  
376 intestinal lumen; therefore, some studies require advanced techniques such as microinjection [47, 48]. Owing to the  
377 3D organoid structure, several organoid culture models have been reported to modify the 3D culture method according  
378 to the purpose of the study [20, 49-51]. For example, when comparing physical indicators, such as permeability  
379 measurements, the structure of organoids affects the outcome of study. Some receptors that regulate the physical  
380 function of intestinal epithelium exist in the apical membrane of epithelial cells. Thus, 3D organoid may not suitable  
381 model to understand regulatory response of gut permeability induced by receptors [52]. In this study, we developed a  
382 pig 2D organoid model and compared it with a pig 3D organoid model, focusing on nutritional perspectives.  
383 Surprisingly, the 2D organoid model had *CHGA* and *ALPI*, which are related to nutrient processing, and when fully  
384 developed, their expression levels are significantly higher than those of the 3D organoid model. Furthermore, the  
385 expression of most nutrient transporter genes was higher in 2D pig organoids. In line with this, many gastrointestinal  
386 hormones and digestive enzyme genes were highly expressed on the pig 2D organoid model. These results suggest  
387 that pig 2D intestinal organoid models not only have structural and characteristic advantages in nutrition-related  
388 studies, but also have superior potential for nutritional physiological responses.

389 As gene expression levels have limited information, we further attempted to confirm the functional activity of  
390 nutrient processing and related response by comparing 3D and 2D pig organoids. We compared the nutrient absorption  
391 of two pig organoid models using a fluorescent fatty acid analog. Fluorescent-conjugated nutrients are widely used in  
392 studies of nutrient uptake in organoids for intestinal function research [53, 54]. Basic organoid cultures have an apical  
393 membrane formed inward, similar to the actual intestinal shape, and these structures may affect uptake in the intestinal  
394 lumen. Therefore, studies on physiological phenomena such as nutrient uptake and drug absorption have reported  
395 changes in the culture methods of intestinal organoids [54, 55]. In previous study, differences in nutrient uptake  
396 according to organoid culture method have been reported [56]. An apical-out culture method, which exposed the apical  
397 side of the intestinal epithelium that absorbs nutrients from the outside, absorbed more nutrients (including fatty acid,  
398 amino acid, and glucose) than organoids of the conventional method. Thus, structural property of organoid models  
399 should be considered for conducting nutritional study. Compared with the pig 3D organoid model, we found that the  
400 pig 2D organoid model absorbed more fatty acids during the same period. Although the exposed apical membrane of  
401 the 2D intestinal organoid model facilitate the absorption of fatty acids, nutrients can be diffused or actively  
402 transported depending on their type, and the degree of uptake can vary depending on the location of nutrient



403 transporters (basal, apical, or both) [57]. Therefore, suitable culture models for target nutrients should be considered  
404 in future organoid-based nutritional studies.

405 Fatty acids, one of the major nutrients, are broken down from dietary lipids in the intestine and absorbed mainly by  
406 enterocytes. Fatty acid metabolism involves several proteins including receptors, transporters, and binding proteins  
407 [58]. Unlike other nutrients, fatty acid absorption pathways exhibit unique properties. First, fatty acids are re-esterified  
408 by related complex molecules before entering enterocytes through the apical membrane. The absorbed fatty acids are  
409 then packaged into pre-chylomicrons or stored as intracellular lipid droplets for fatty acid oxidation. Finally, mature  
410 chylomicrons are released from the enterocytes and transported throughout the body via the lymphatic system [59].  
411 Nutrients can induce various signals in the gastrointestinal tract, including peptide hormone release by enteroendocrine  
412 cells. These hormones act efficiently over the short term and are secreted by several types of enteroendocrine cells  
413 that secrete hormones such as glucagon-like peptide 1 and 2 (GLP-1 and GLP-2), cholecystokinin (CCK), glucose-  
414 dependent insulinotropic polypeptide (GIP), and peptide YY (PYY) [42]. As an example of hormone release by fatty  
415 acids, it has been reported that LCFAs significantly induce the release of GLP-1 and GLP-2 in the pig gut tissue ex  
416 vivo culture model [60]. To confirm the response to fatty acids, especially LCFAs, in pig intestinal organoid models,  
417 we compared the gene expression levels of fatty acid metabolism-related proteins and hormones after treatment with  
418 LM. In summary, no significant differences were found in the 3D organoid model; however, in the 2D organoid model,  
419 the LCFA receptor and several hormone-encoding genes showed an overall increase after LM treatment. FFAR1 and  
420 FFAR4 (as well-known GPR 40 and GPR120, respectively) are representative LCFA receptors as types of G protein-  
421 coupled receptor (GPCR). And they that are expressed in several enteroendocrine cell types and are associated with  
422 hormones [61]. Some gut hormones, including CCK, GLP-1, and PYY, are well known for their anorexic activity, in  
423 which their concentrations rise soon after food ingestion and remain elevated for up to several hours, depending on  
424 meal size and composition [62]. Lipid intake in food stimulates the release of these hormones and increases their  
425 plasma concentrations [63, 64]. To support the association between receptors and hormones, deficient mouse models  
426 of FFAR1 or FFAR4 have been shown to impair lipid-induced hormone secretion responses [65, 66]. Our 2D pig  
427 intestinal organoid model suggested that fatty acids can be recognized by receptors in the apical membrane and can  
428 simulate hormonal responses similar to those in the intestinal lumen. However, since there are limitations due to  
429 comparisons at the genetic level, it is necessary to directly compare hormone secretion levels or study the mechanism  
430 of the intracellular fatty acid-induced pathway up to hormone release.

431 LCFAs can be divided into saturated and unsaturated fatty acids based on their 12–20 carbon chain composition.  
432 LCFAs absorbed by cells are regulated by several metabolic responses, including cellular metabolism, energy  
433 homeostasis, and cell proliferation [67]. Various LCFAs, like other nutrients, can diffuse or be transferred through  
434 specific proteins. First, LCFAs uptake is carried out by plasma membrane-associated fatty acid-binding protein  
435 (FABPpm) such as fatty acid transport protein 4 (FATP4), and cluster of differentiation 36 (CD36) in enterocytes.  
436 LCFAs absorbed by acyl-CoA synthetase (ASC) are present as free fatty acids or fatty acyl coenzyme A (fatty acyl-  
437 CoA). They are then bound by fatty acid-binding protein (FABP) and acyl-CoA binding protein (ACBP) and trafficked  
438 into the cells [68]. Fatty acyl-CoA migrates to the mitochondria, and intramitochondrial oxidation proceeds via the  
439 beta oxidation pathway. The mitochondrial matrix does not contain enzymes that activate fatty acids containing 14 or  
440 more carbon atoms. Thus, the entry of LCFAs into the mitochondria is regulated by specific enzyme activities, such  
441 as carnitine palmitoyltransferase 1 (CPT 1) and CPT 2. Acetyl coenzyme A (acetyl-CoA) is produced as an end product  
442 of beta oxidation, and it promotes ATP synthesis through the tricarboxylic acid (TCA) cycle [69]. To confirm LCFAs-  
443 induced metabolism in pig organoid models, mitochondria staining and intracellular ADP:ATP ratios were compared.  
444 In our study, LM treatment increased mitochondrial fluorescence intensity in 2D organoids but not in 3D organoids.  
445 In addition, there was no significant difference in the ADP:ATP ratio after LM treatment in 3D organoids, whereas it  
446 decreased in 2D organoids. The ADP:ATP ratio reduction may imply the presence of a larger proportion of ATP  
447 within the cells, which, together with the mitochondria staining results, may have contributed to the generation of  
448 ATP through fatty acid oxidation within the 2D organoids. However, no changes were observed in 3D organoids,  
449 which may have caused poor fatty acid transfer into the cells or differences in fatty acid oxidation-related enzyme  
450 activity. Collectively, 2D and 3D organoid systems show different physiological response in nutrient metabolism  
451 maybe due to poor nutrient absorption and/or lower expression of nutrient process-related cells and gene expression.

452

453

## Conclusion

454 In summary, our results suggested that pig intestinal organoids are more suitable for intestinal epithelial cell research  
455 than the existing in vitro systems such as IPEC-J2. Furthermore, we have established a 2D organoid model for  
456 intestinal lumen research and further compared nutrient-related properties, such as nutrient transporters, hormones,  
457 and digestive enzymes, with a 3D organoid model to characterize them. Compared with the 3D organoid model, the  
458 established 2D organoid model showed more active absorption of nutrients, gene expression, and metabolic processes  
459 related to nutrient responses. These findings emphasize the suitability of the 2D organoid model as an in vitro platform

460 for nutrition-related research and provide an improved understanding of nutrient use by intestinal epithelial cells. This  
461 study provides essential information for further investigations of the interactions between intestinal epithelial cells  
462 and nutrients in the gut environment.

463

464

### **Acknowledgments**

465 The authors thank technical and financial support from all members of the Application Center at the CJ Blossom Park  
466 (Suwon, Republic of Korea).

467

468

ACCEPTED

## References

- 470 1. Maes DG, Dewulf J, Piñeiro C, Edwards S, Kyriazakis I. A critical reflection on intensive pork production with  
471 an emphasis on animal health and welfare. *J Anim Sci.* 2020;98(Supplement\_1):S15-S26.  
472 <https://doi.org/10.1093/jas/skz362>
- 473 2. Kim KY, Ko HJ, Kim HT, Kim CN, Byeon SH. Association between pig activity and environmental factors in  
474 pig confinement buildings. *Aust J Exp Agric.* 2008;48(5):680-6. <https://doi.org/10.1071/EA06110>
- 475 3. Rutherford K, Baxter E, D'eath R, Turner S, Arnott G, Roehe R, et al. The welfare implications of large litter  
476 size in the domestic pig I: biological factors. *Anim Welf.* 2013;22(2):199-218.  
477 <https://doi.org/10.7120/09627286.22.2.199>
- 478 4. Lallès JP, Bosi P, Smidt H, Stokes CR. Nutritional management of gut health in pigs around weaning. *Proc Nutr*  
479 *Soc.* 2007;66(2):260-8. <https://doi.org/10.1017/S0029665107005484>
- 480 5. Che L, Zhou Q, Liu Y, Hu L, Peng X, Wu C, et al. Flaxseed oil supplementation improves intestinal function  
481 and immunity, associated with altered intestinal microbiome and fatty acid profile in pigs with intrauterine growth  
482 retardation. *Food Funct.* 2019;10(12):8149-60. <https://doi.org/10.1039/C9FO01877H>
- 483 6. Saleri R, Borghetti P, Ravanetti F, Cavalli V, Ferrari L, De Angelis E, et al. Effects of different short-chain fatty  
484 acids (SCFA) on gene expression of proteins involved in barrier function in IPEC-J2. *Porcine Health Manag.*  
485 2022;8(1):21. <https://doi.org/10.1186/s40813-022-00264-z>
- 486 7. Du Y, Li X, Niu Q, Mo X, Qui M, Ma T, et al. Development of a miniaturized 3D organoid culture platform for  
487 ultra-high-throughput screening. *J Mol Cell Biol.* 2020;12(8):630-43. <https://doi.org/10.1093/jmcb/mjaa036>
- 488 8. Hou Q, Ye L, Liu H, Huang L, Yang Q, Turner J, et al. Lactobacillus accelerates ISCs regeneration to protect the  
489 integrity of intestinal mucosa through activation of STAT3 signaling pathway induced by LPLs secretion of IL-  
490 22. *Cell Death Differ.* 2018;25(9):1657-70. <https://doi.org/10.1038/s41418-018-0070-2>
- 491 9. Clevers H. Modeling development and disease with organoids. *Cell.* 2016;165(7):1586-97.
- 492 10. Rossi G, Manfrin A, Lutolf MP. Progress and potential in organoid research. *Nat Rev Genet.* 2018;19(11):671-  
493 87. <https://doi.org/10.1016/j.cell.2016.05.082>
- 494 11. Rookmaaker MB, Schutgens F, Verhaar MC, Clevers H. Development and application of human adult stem or  
495 progenitor cell organoids. *Nature Reviews Nephrology.* 2015;11(9):546-54.  
496 <https://doi.org/10.1038/nrneph.2015.118>
- 497 12. Kawasaki M, Goyama T, Tachibana Y, Nagao I, Ambrosini YM. Farm and companion animal organoid models  
498 in translational research: a powerful tool to bridge the gap between mice and humans. *Front Med Technol.*  
499 2022;4:895379. <https://doi.org/10.3389/fmedt.2022.895379>
- 500 13. Sato T, Stange DE, Ferrante M, Vries RG, Van Es JH, Van Den Brink S, et al. Long-term expansion of epithelial

- 501 organoids from human colon, adenoma, adenocarcinoma, and Barrett's epithelium. *Gastroenterology*.  
502 2011;141(5):1762-72. <https://doi.org/10.1053/j.gastro.2011.07.050>
- 503 14. Blake R, Jensen K, Mabbott N, Hope J, Stevens J. The development of 3D bovine intestinal organoid derived  
504 models to investigate *Mycobacterium avium* ssp *paratuberculosis* pathogenesis. *Front Vet Sci*. 2022;9:921160.  
505 <https://doi.org/10.3389/fvets.2022.921160>
- 506 15. Smith D, Price DR, Burrells A, Faber MN, Hildersley KA, Chintoan-Uta C, et al. The development of ovine  
507 gastric and intestinal organoids for studying ruminant host-pathogen interactions. *Front Cell Infect Microbiol*.  
508 2021;11:733811. <https://doi.org/10.3389/fcimb.2021.733811>
- 509 16. Li J, Li Jr J, Zhang S, Li R, Lin X, Mi Y, et al. Culture and characterization of chicken small intestinal crypts.  
510 *Poult Sci*. 2018;97(5):1536-43. <https://doi.org/10.3382/ps/pey010>
- 511 17. Gonzalez LM, Williamson I, Piedrahita JA, Blikslager AT, Magness ST. Cell lineage identification and stem cell  
512 culture in a porcine model for the study of intestinal epithelial regeneration. *PloS One*. 2013;8(6):e66465.  
513 <https://doi.org/10.1371/journal.pone.0066465>
- 514 18. Derricott H, Luu L, Fong WY, Hartley CS, Johnston LJ, Armstrong SD, et al. Developing a 3D intestinal  
515 epithelium model for livestock species. *Cell Tissue Res*. 2019;375:409-24. <https://doi.org/10.1007/s00441-018-2924-9>
- 517 19. Li Y, Yang N, Chen J, Huang X, Zhang N, Yang S, et al. Next-generation porcine intestinal organoids: an apical-  
518 out organoid model for swine enteric virus infection and immune response investigations. *J Virol*.  
519 2020;94(21):10.1128/jvi.01006-20. <https://doi.org/10.1128/jvi.01006-20>
- 520 20. Joo SS, Gu BH, Park YJ, Rim CY, Kim MJ, Kim SH, et al. Porcine intestinal apical-out organoid model for gut  
521 function study. *Animals (Basel)*. 2022;12(3):372. <https://doi.org/10.3390/ani12030372>
- 522 21. Schmittgen TD, Livak KJ. Analyzing real-time PCR data by the comparative CT method. *Nat Protoc*.  
523 2008;3(6):1101-8. <https://doi.org/10.1038/nprot.2008.73>
- 524 22. Ahlman H, Nilsson O. The gut as the largest endocrine organ in the body. *Ann Oncol*. 2001;12:S63-S8.  
525 [https://doi.org/10.1093/annonc/12.suppl\\_2.S63](https://doi.org/10.1093/annonc/12.suppl_2.S63)
- 526 23. Ohno T, Mochiki E, Kuwano H. The roles of motilin and ghrelin in gastrointestinal motility. *Int J of Pept*.  
527 2010;2010(1):820794. <https://doi.org/10.1155/2010/820794>
- 528 24. Chelakkot C, Ghim J, Ryu SH. Mechanisms regulating intestinal barrier integrity and its pathological  
529 implications. *Exp Mol Med*. 2018;50(8):1-9. <https://doi.org/10.1038/s12276-018-0126-x>
- 530 25. Peterson LW, Artis D. Intestinal epithelial cells: regulators of barrier function and immune homeostasis. *Nat Rev*  
531 *Immunol*. 2014;14(3):141-53. <https://doi.org/10.1038/nri3608>

- 532 26. De Santa Barbara P, Van Den Brink GR, Roberts DJ. Development and differentiation of the intestinal epithelium.  
533 Cell Mol Life Sci. 2003;60:1322-32. <https://doi.org/10.1007/s00018-003-2289-3>
- 534 27. Malagola E, Vasciaveo A, Ochiai Y, Kim W, Zheng B, Zanella L, et al. Isthmus progenitor cells contribute to  
535 homeostatic cellular turnover and support regeneration following intestinal injury. Cell. 2024;187(12):3056-71.  
536 e17. <https://doi.org/10.1016/j.cell.2024.05.004>
- 537 28. Iglesias DE, Cremonini E, Fraga CG, Oteiza PI. Ellagic acid protects Caco-2 cell monolayers against  
538 inflammation-induced permeabilization. Free Radic Biol Med. 2020;152:776-86.  
539 <https://doi.org/10.1016/j.freeradbiomed.2020.01.022>
- 540 29. Larraufie P, Martin-Gallausiaux C, Lapaque N, Dore J, Gribble F, Reimann F, et al. SCFAs strongly stimulate  
541 PYY production in human enteroendocrine cells. Sci Rep. 2018;8(1):74. <https://doi.org/10.1038/s41598-017-18259-0>  
542
- 543 30. Yang F, Wang A, Zeng X, Hou C, Liu H, Qiao S. Lactobacillus reuteri I5007 modulates tight junction protein  
544 expression in IPEC-J2 cells with LPS stimulation and in newborn piglets under normal conditions. BMC  
545 microbiol. 2015;15:1-11. <https://doi.org/10.1186/s12866-015-0372-1>
- 546 31. Kaur G, Dufour JM. Cell lines: Valuable tools or useless artifacts. Spermatogenesis. 2012;2(1):1-5.  
547 <https://doi.org/10.4161/spmg.19885>
- 548 32. Sato T, Vries RG, Snippert HJ, Van De Wetering M, Barker N, Stange DE, et al. Single Lgr5 stem cells build  
549 crypt-villus structures in vitro without a mesenchymal niche. Nature. 2009;459(7244):262-5.  
550 <https://doi.org/10.1038/nature07935>
- 551 33. Fujii M, Matano M, Toshimitsu K, Takano A, Mikami Y, Nishikori S, et al. Human intestinal organoids maintain  
552 self-renewal capacity and cellular diversity in niche-inspired culture condition. Cell stem cell. 2018;23(6):787-  
553 93. e6. <https://doi.org/10.1016/j.stem.2018.11.016>
- 554 34. Yin YB, Guo SG, Wan D, Wu X, Yin YL. Enteroids: promising in vitro models for studies of intestinal  
555 physiology and nutrition in farm animals. J Agric Food Chem. 2019;67(9):2421-8.  
556 <https://doi.org/10.1021/acs.jafc.8b06908>
- 557 35. Seeger B. Farm animal-derived models of the intestinal epithelium: recent advances and future applications of  
558 intestinal organoids. Altern Lab Anim. 2020;48(5-6):215-33. <https://doi.org/10.1177/026119292097402>
- 559 36. Li XG, Zhu M, Chen MX, Fan HB, Fu HL, Zhou JY, et al. Acute exposure to deoxynivalenol inhibits porcine  
560 enteroid activity via suppression of the Wnt/ $\beta$ -catenin pathway. Toxicol Lett. 2019;305:19-31.  
561 <https://doi.org/10.1016/j.toxlet.2019.01.008>
- 562 37. Mitchell J, Sutton K, Elango JN, Borowska D, Perry F, Lahaye L, et al. Chicken intestinal organoids: a novel  
563 method to measure the mode of action of feed additives. Front Immunol. 2024;15:1368545.  
564 <https://doi.org/10.3389/fimmu.2024.1368545>

- 565 38. Brosnahan AJ, Brown DR. Porcine IPEC-J2 intestinal epithelial cells in microbiological investigations. *Vet*  
566 *Microbiol.* 2012;156(3-4):229-37. <https://doi.org/10.1016/j.vetmic.2011.10.017>
- 567 39. Zakrzewski SS, Richter JF, Krug SM, Jebautzke B, Lee IFM, Rieger J, et al. Improved cell line IPEC-J2,  
568 characterized as a model for porcine jejunal epithelium. *PloS one.* 2013;8(11):e79643.  
569 <https://doi.org/10.1371/journal.pone.0079643>
- 570 40. Günzel D, Fromm M. Claudins and other tight junction proteins. *Compr Physiol.* 2012;2(3):1819-52.  
571 <https://doi.org/10.1002/cphy.c110045>
- 572 41. Van der Hee B, Madsen O, Vervoort J, Smidt H, Wells JM. Congruence of transcription programs in adult stem  
573 cell-derived jejunum organoids and original tissue during long-term culture. *Front Cell Dev Biol.* 2020;8:529393.  
574 <https://doi.org/10.3389/fcell.2020.00375>
- 575 42. Gribble FM, Reimann F. Enteroendocrine cells: chemosensors in the intestinal epithelium. *Annu Rev Physiol.*  
576 2016;78(1):277-99. <https://doi.org/10.1146/annurev-physiol-021115-105439>
- 577 43. Wang Y, Song W, Wang J, Wang T, Xiong X, Qi Z, et al. Single-cell transcriptome analysis reveals differential  
578 nutrient absorption functions in human intestine. *J Exp Med.* 2020;217(2). <https://doi.org/10.1084/jem.20191130>
- 579 44. McCauley HA. Enteroendocrine regulation of nutrient absorption. *J Nutr.* 2020;150(1):10-21.  
580 <https://doi.org/10.1093/jn/nxz191>
- 581 45. Zietek T, Rath E, Haller D, Daniel H. Intestinal organoids for assessing nutrient transport, sensing and incretin  
582 secretion. *Sci Rep.* 2015;5(1):16831. <https://doi.org/10.1038/srep16831>
- 583 46. Sauvanet C, Wayt J, Pelaseyed T, Bretscher A. Structure, regulation, and functional diversity of microvilli on the  
584 apical domain of epithelial cells. *Annu Rev Cell Dev Biol.* 2015;31(1):593-621. [https://doi.org/10.1146/annurev-  
cellbio-100814-125234](https://doi.org/10.1146/annurev-<br/>585 cellbio-100814-125234)
- 586 47. Williamson IA, Arnold JW, Samsa LA, Gaynor L, DiSalvo M, Cocchiaro JL, et al. A high-throughput organoid  
587 microinjection platform to study gastrointestinal microbiota and luminal physiology. *Cell Mol Gastroenterol*  
588 *Hepatol.* 2018;6(3):301-19. <https://doi.org/10.1016/j.jcmgh.2018.05.004>
- 589 48. Hill DR, Huang S, Tsai YH, Spence JR, Young VB. Real-time measurement of epithelial barrier permeability in  
590 human intestinal organoids. *J Vis Exp.* 2017(130):e56960. <https://doi.org/10.3791/56960>
- 591 49. Kar SK, Van Der Hee B, Loonen LM, Taverner N, Taverner-Thiele JJ, Schokker D, et al. Effects of undigested  
592 protein-rich ingredients on polarised small intestinal organoid monolayers. *J Anim Sci Biotechnol.* 2020;11:1-7.  
593 <https://doi.org/10.1186/s40104-020-00443-4>
- 594 50. Wright CW, Li N, Shaffer L, Hill A, Boyer N, Alves SE, et al. Establishment of a 96-well transwell system using  
595 primary human gut organoids to capture multiple quantitative pathway readouts. *Sci Rep.* 2023;13(1):16357.  
596 <https://doi.org/10.1038/s41598-023-43656-z>

- 597 51. Kasendra M, Tovagliari A, Sontheimer-Phelps A, Jalili-Firoozinezhad S, Bein A, Chalkiadaki A, et al.  
598 Development of a primary human Small Intestine-on-a-Chip using biopsy-derived organoids. *Sci Rep.*  
599 2018;8(1):1-14. <https://doi.org/10.1038/s41598-018-21201-7>
- 600 52. Bardenbacher M, Ruder B, Britzen-Laurent N, Schmid B, Waldner M, Naschberger E, et al. Permeability  
601 analyses and three dimensional imaging of interferon gamma-induced barrier disintegration in intestinal  
602 organoids. *Stem Cell Res.* 2019;35:101383. <https://doi.org/10.1016/j.scr.2019.101383>
- 603 53. Margalef-Català M, Li X, Mah AT, Kuo CJ, Monack DM, Amieva MR. Controlling epithelial polarity: a human  
604 enteroid model for host-pathogen interactions. *Cell Rep.* 2019;26(9):2509-20. e4.  
605 <https://doi.org/10.1016/j.celrep.2019.01.108>
- 606 54. Zhang W, Tian Y, Chen B, Xu S, Wu L. PFOA/PFOS Facilitated Intestinal Fatty Acid Absorption by Activating  
607 the PPAR $\alpha$  Pathway: Insights from Organoids Model. *Environ Health (Wash).* 2023;2(2):85-94.  
608 <https://doi.org/10.1021/envhealth.3c00129>
- 609 55. Li D, Rodia CN, Johnson ZK, Bae M, Muter A, Heussinger AE, et al. Intestinal basolateral lipid substrate  
610 transport is linked to chylomicron secretion and is regulated by apoC-III. *J Lipid Res.* 2019;60(9):1503-  
611 15. <https://doi.org/10.1194/jlr.M092460>
- 612 56. Kang TH, Lee SI. Establishment of a chicken intestinal organoid culture system to assess deoxynivalenol-induced  
613 damage of the intestinal barrier function. *J Anim Sci Biotechnol.* 2024;15(1):30. <https://doi.org/10.1186/s40104-023-00976-4>
- 615 57. Duca FA, Waise TZ, Pepler WT, Lam TK. The metabolic impact of small intestinal nutrient sensing. *Nat*  
616 *Commun.* 2021;12(1):903. <https://doi.org/10.1038/s41467-021-21235-y>
- 617 58. Gajda AM, Storch J. Enterocyte fatty acid-binding proteins (FABPs): different functions of liver and intestinal  
618 FABPs in the intestine. *Prostaglandins Leukot Essent Fatty Acids.* 2015;93:9-16.  
619 <https://doi.org/10.1016/j.plefa.2014.10.001>
- 620 59. Ko CW, Qu J, Black DD, Tso P. Regulation of intestinal lipid metabolism: current concepts and relevance to  
621 disease. *Nat Rev Gastroenterol Hepatol.* 2020;17(3):169-83. <https://doi.org/10.1038/s41575-019-0250-7>
- 622 60. Voortman T, Hendriks HF, Witkamp RF, Wortelboer HM. Effects of long-and short-chain fatty acids on the  
623 release of gastrointestinal hormones using an ex vivo porcine intestinal tissue model. *J Agric Food Chem.*  
624 2012;60(36):9035-42. <https://doi.org/10.1021/jf2045697>
- 625 61. Grundmann M, Bender E, Schamberger J, Eitner F. Pharmacology of free fatty acid receptors and their allosteric  
626 modulators. *Int J Mol Sci.* 2021;22(4):1763. <https://doi.org/10.3390/ijms22041763>
- 627 62. Gribble FM, Reimann F. Function and mechanisms of enteroendocrine cells and gut hormones in metabolism.  
628 *Nat Rev Endocrinol.* 2019;15(4):226-37. <https://doi.org/10.1038/s41574-019-0168-8>
- 629 63. Ekberg JH, Hauge M, Kristensen LV, Madsen AN, Engelstoft MS, Husted AS, et al. GPR119, a major



- 630 enteroendocrine sensor of dietary triglyceride metabolites coacting in synergy with FFA1 (GPR40).  
631 *Endocrinology*. 2016;157(12):4561-9. <https://doi.org/10.1210/en.2016-1334>
- 632 64. Mandøe MJ, Hansen KB, Windeløv JA, Knop FK, Rehfeld JF, Rosenkilde MM, et al. Comparing olive oil and  
633 C4-dietary oil, a prodrug for the GPR119 agonist, 2-oleoyl glycerol, less energy intake of the latter is needed to  
634 stimulate incretin hormone secretion in overweight subjects with type 2 diabetes. *Nutr Diabetes*. 2018;8(1):2.  
635 <https://doi.org/10.1038/s41387-017-0011-z>
- 636 65. Iwasaki K, Harada N, Sasaki K, Yamane S, Iida K, Suzuki K, et al. Free fatty acid receptor GPR120 is highly  
637 expressed in enteroendocrine K cells of the upper small intestine and has a critical role in GIP secretion after fat  
638 ingestion. *Endocrinology*. 2015;156(3):837-46. <https://doi.org/10.1210/en.2014-1653>
- 639 66. Liou AP, Lu X, Sei Y, Zhao X, Pechhold S, Carrero RJ, et al. The G-protein– coupled receptor GPR40 directly  
640 mediates long-chain fatty acid– induced secretion of cholecystokinin. *Gastroenterology*. 2011;140(3):903-12. e4.  
641 <https://doi.org/10.1053/j.gastro.2010.10.012>
- 642 67. He Q, Chen Y, Wang Z, He H, Yu P. Cellular uptake, metabolism and sensing of long-chain fatty acids. *Front*  
643 *Biosci (Landmark Ed)*. 2023;28(1):10. <https://doi.org/10.31083/j.fbl2801010>
- 644 68. Niot I, Poirier H, Tran TTT, Besnard P. Intestinal absorption of long-chain fatty acids: evidence and uncertainties.  
645 *Prog Lipid Res*. 2009;48(2):101-15. <https://doi.org/10.1016/j.plipres.2009.01.001>
- 646 69. Nguyen P, Leray V, Diez M, Serisier S, Bloc'h JL, Siliart B, et al. Liver lipid metabolism. *J Anim Physiol Anim*  
647 *Nutr (Berl)*. 2008;92(3):272-83. <https://doi.org/10.1111/j.1439-0396.2007.00752.x>

648

ACCEPTED

649

(A)

## Tables and Figures

650

651

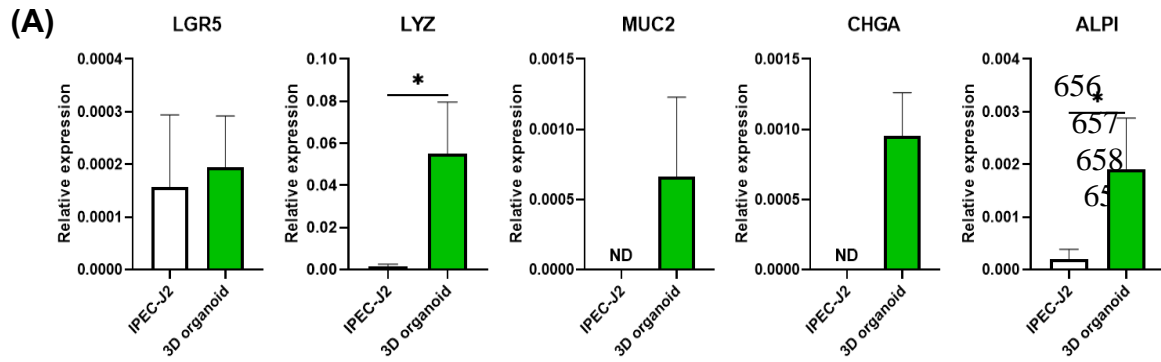
Table 1. List of primers in this study

Gene	Description	Forward	Reverse	Size (base pair)
<i>LGR5</i>	Leucine-rich repeat-containing G-protein coupled receptor 5	CCTTGGCCCTGAACAAAATA	ATTTCTTTCCAGGGAGTGG	110
<i>LYZ</i>	Lysozyme	GCAAGACACCCAAAGCAGTT	ATGCCACCCATGCTTTAACG	132
<i>MUC2</i>	Mucin 2	GCTGGCCGACAACAAGAAGA	TGGTGGGAGGATGGTTGGAA	126
<i>CHGA</i>	Chromogranin-A	TGAAGTGCATCGTCGAGGTC	GAGGATCCGTTTCATCTCCTCG	104
<i>ALPI</i>	Alkaline Phosphatase, Intestinal	AGGAACCCAGAGGGACCATTTC	CACAGTGGCTGAGGGACTTAGG	83
<i>SGLT1</i>	Sodium/glucose cotransporter 1	GTCGTCTCCCTCTTACCAAG	ATGGTCTCTTCTGGGGCTTCT	137
<i>GLUT2</i>	Glucose transporter 2	CCAGGCCCATCCCTGGTT	GCGGGTCCAGTGTGAATGC	96
<i>GLUT5</i>	Glucose transporter 5	CCCAGGAGCCGGTCAAG	TCAGCGTCGCCAAAGCA	60
<i>PEPT1</i>	Peptide transporter 1	TTCTAAGCAGCCAGCCATGAA	CCAGTGTGTGTGTGTGTGTG	119
<i>CD36</i>	Cluster of differentiation 36	GGAGAAAAGATCACTACCATCA TGAG	CTCCTGAAGTCAATGTA ACTGAC A	78
<i>GAST</i>	Gastrin	TGGATGGAGGAGGAAGAAGAAG	TGGCTTTCATGTGGCTGGA	142
<i>CCK</i>	Cholecystokinin	CAGGCTCGAAAAGCACCTTC	GCGGGTCTTCTAGGAGGTA	157
<i>GCG</i>	Proglucagon	AGAACTCCGCCGAGACA	TAAAGTCTCGGGTGGCAAGATT	83
<i>GIP</i>	Gastric Inhibitory Polypeptide	GGACAAGATCCGCCAACAAAGA	CTCGCTCCTCCTTCCTGTTA	141
<i>SST</i>	Somatostatin	CCCAACCAGACAGAGAACGAT	GGCCGGTTTGAGTTAGCT	108
<i>MLN</i>	Motilin	CCAGAATGCCGCAAGTAACA	GCTGTTGGGAGAGGGTGT	124
<i>GHRL</i>	Ghrelin	AAGAAGCCAGCAGCCAAACT	GACTGAGCCCCTGACAACT	149
<i>PYY</i>	Peptide YY	ACTCTCTCGCCTTCCATTTT	AGTGTCCCCAGGCAGATGA	127
<i>SI</i>	Sucrase-isomaltase	GGCCATGGAGAAAACAACGT	TCGGCTGGCAGTTGTAGTTA	119
<i>MGAM</i>	Maltase-glucoamylase	TCATCATCTCTCGCTCCACC	GGCTAAACTCCATCATGCCG	120
<i>LCT</i>	Lactase	ACAATGCCACTGGAGACGTA	GAAAACCCGAGACCAGGAGA	119
<i>DPEP1</i>	Dipeptidase 1	GAGCGTCGTGAAGGAGATGAA	CGAGGAGTGGCTGAAGATGAC	121
<i>ANPEP</i>	Alanyl aminopeptidase	ACATCTACCCACTCCCCAAA	TCGCTCTTTGTTGCTGATGGA	144
<i>FFAR1</i>	Free fatty acid receptor 1	GAGGCTGGCTGGACAATACTA	AGAAGAACAGGAGAGAGAGGC	132
<i>FFAR4</i>	Free fatty acid receptor 4	GCACCCGTGTACCTGCTTTA	AAGGAACCCACAGCAAATCCTT T	127
<i>FABP1</i>	Fatty acid binding protein 1	GGAAGGACATCAAGGGGACAT	AGTCAGGGTCTCCATCTCACA	131
<i>FABP2</i>	Fatty acid binding protein 2	TTAACTACAGCCTCGCAGACG	CCTCTTGGCTTCTACTCTTCA	176
<i>FABP5</i>	Fatty acid binding protein 5	AGGCACCAGTCCGCTTATTC	GCCATTCCCACTCCTACTTCC	138
<i>GAPDH</i>	Glyceraldehyde-3-phosphate dehydrogenase	ATTCCACCCACGGCAAGTTC	CACCAGCATCACCCATTTG	126

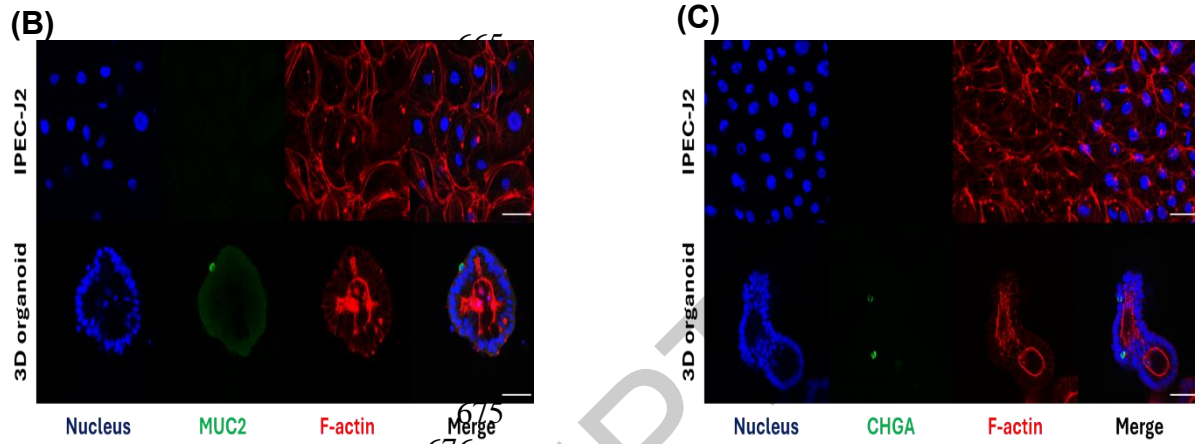
652

653

654  
655



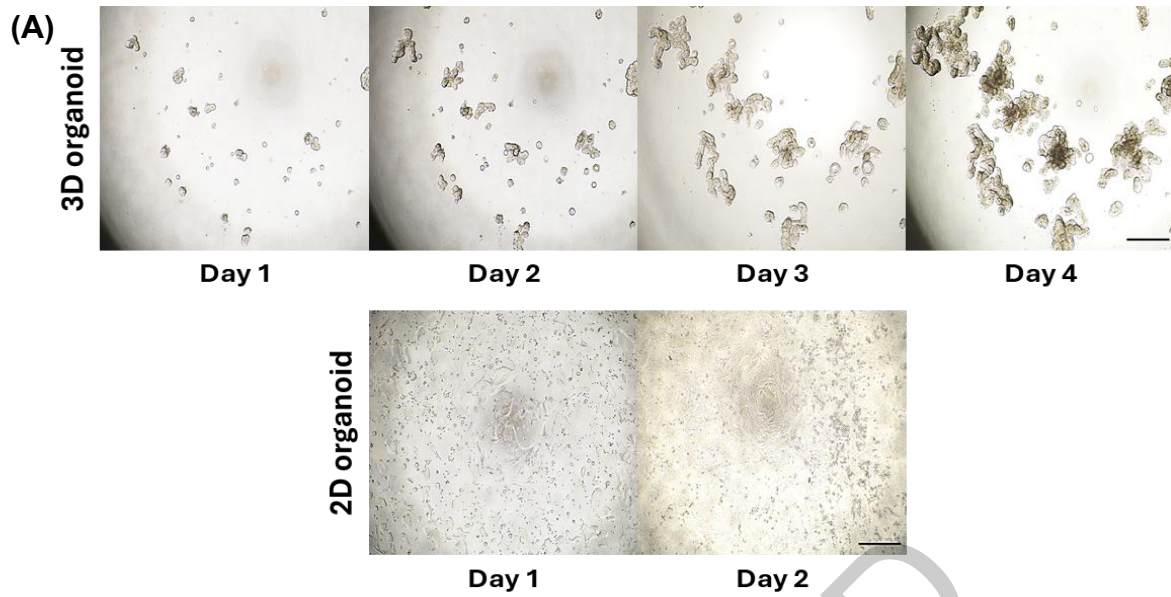
660  
661  
662  
663  
664



677 **Fig. 1 Comparison of IPEC-J2 cell and pig intestinal organoids.** (A) Expression of the mRNA levels of epithelial  
678 cell marker genes in IPEC-J2 and pig intestinal organoids. Data are presented as mean  $\pm$  standard deviation (n = 3-5).  
679 \* $p < 0.05$ , ND; non-detected. (B) Immunostaining of MUC2 in IPEC-J2 and pig intestinal organoids. (C)  
680 Immunostaining of CHGA in IPEC-J2 and pig intestinal organoids. Nucleus and F-actin were stained with Hoechst  
681 33342 and phalloidin. Scale bar = 50  $\mu$ m.

682

683



684

685

686

687

688

689

690

691

692

693

694

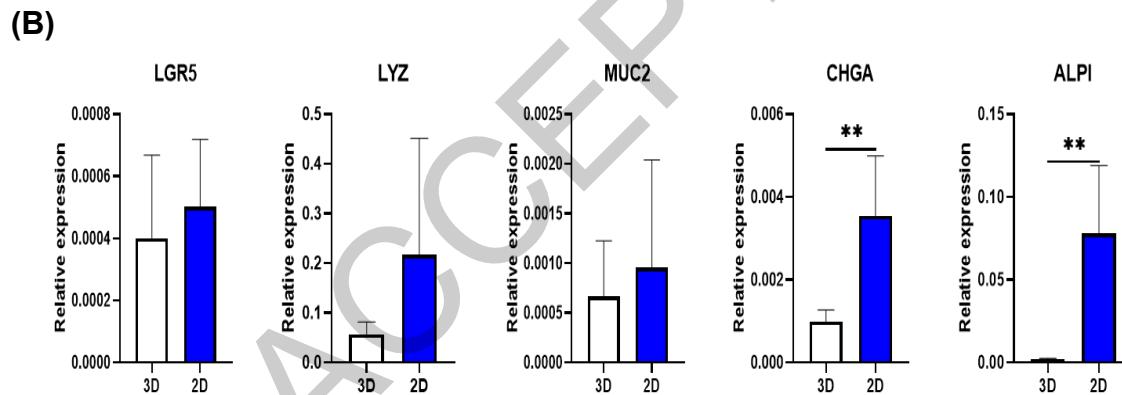
695

696

697

698

699



700

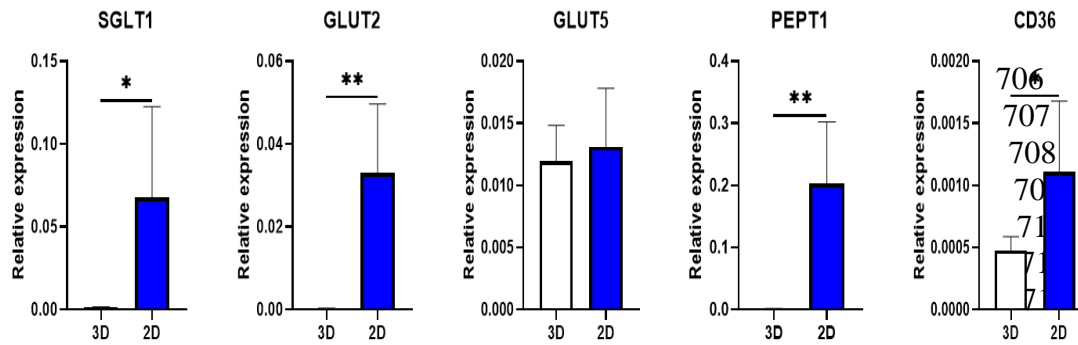
701

702

703

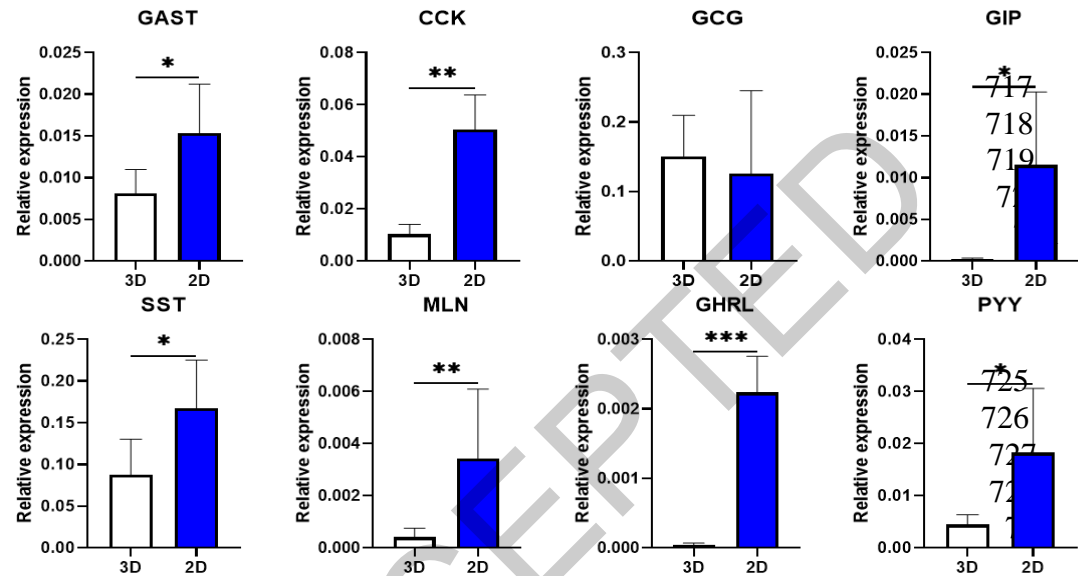
**Fig. 2 Development of 2D pig intestinal organoids.** (A) Representative image of 3D and 2D pig intestinal organoids. Scale bar = 500  $\mu$ m. (B) Expression of the mRNA levels of epithelial cell marker genes in 3D and 2D pig intestinal organoids. Data are presented as mean  $\pm$  standard deviation (n = 5). \*\*  $p < 0.01$ .

704  
705



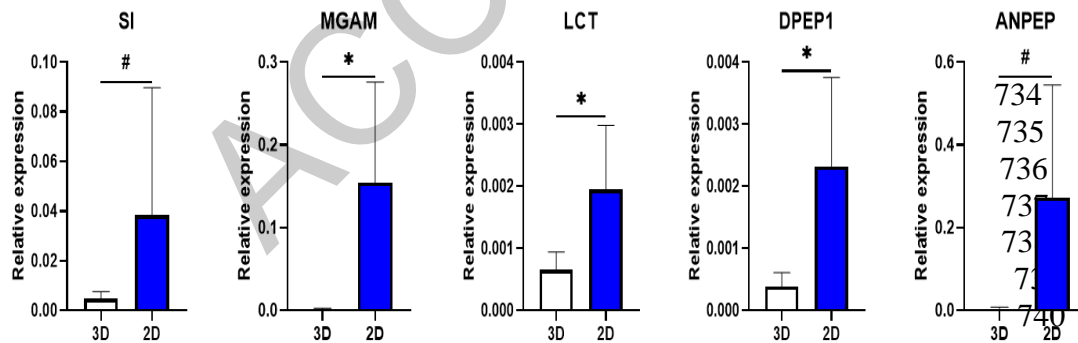
713  
714  
715  
716

(B)



722  
723  
724

(C)



730  
731  
732  
733

741

742

743

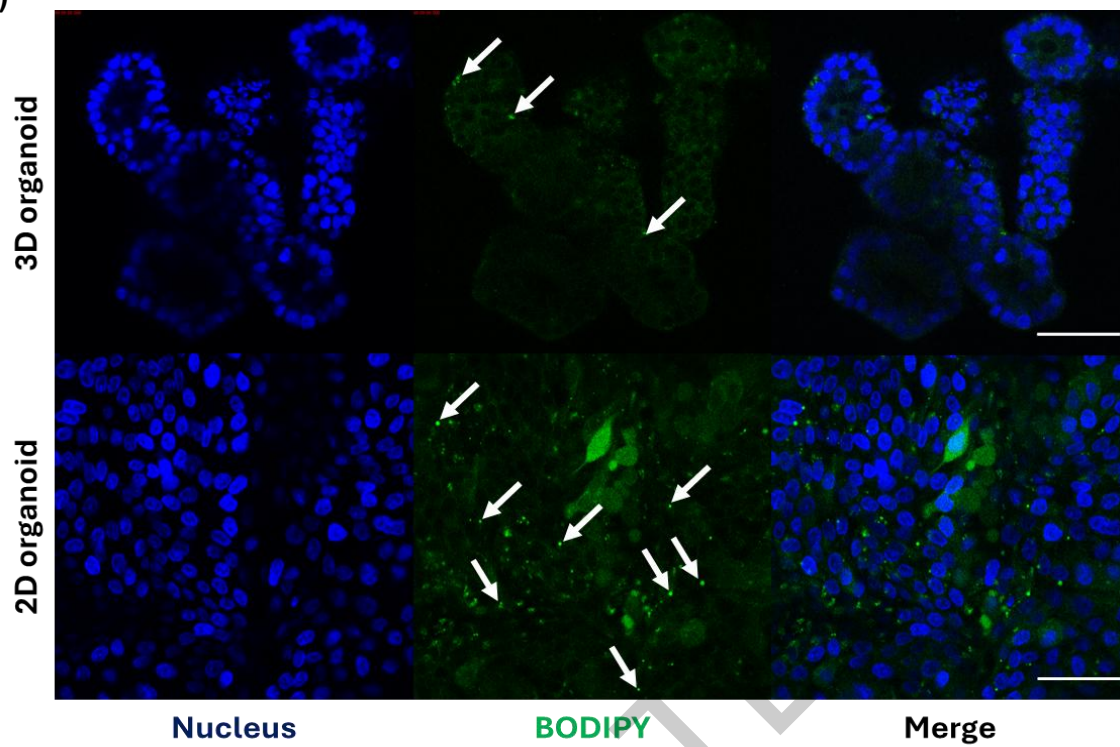
744

745

746

**Fig. 3 Nutrition-related properties of 3D and 2D pig intestinal organoids.** (A) Expression of the mRNA levels of nutrient transporter genes in 3D and 2D pig intestinal organoids. (B) Expression of the mRNA levels of gastrointestinal hormone genes in 3D and 2D pig intestinal organoids. (C) Expression of the mRNA levels of brush border enzyme genes in 3D and 2D pig intestinal organoids. Data are presented as mean  $\pm$  standard deviation ( $n = 5$ ).  $0.05 < \#p < 0.10$ ;  $*p < 0.05$ ;  $**p < 0.01$ ;  $***p < 0.001$ .

(A)



ACCEPTED

748  
749  
750  
751  
752  
753  
754  
755  
756  
757  
758  
759  
760  
761  
762  
763  
764  
765  
766  
767  
768  
769  
770  
771  
772  
773  
774  
775  
776  
777  
778

(B)

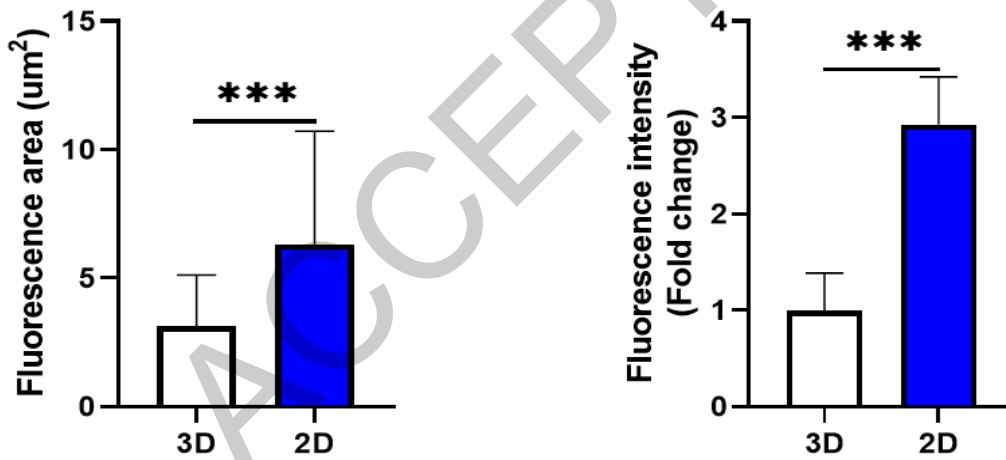
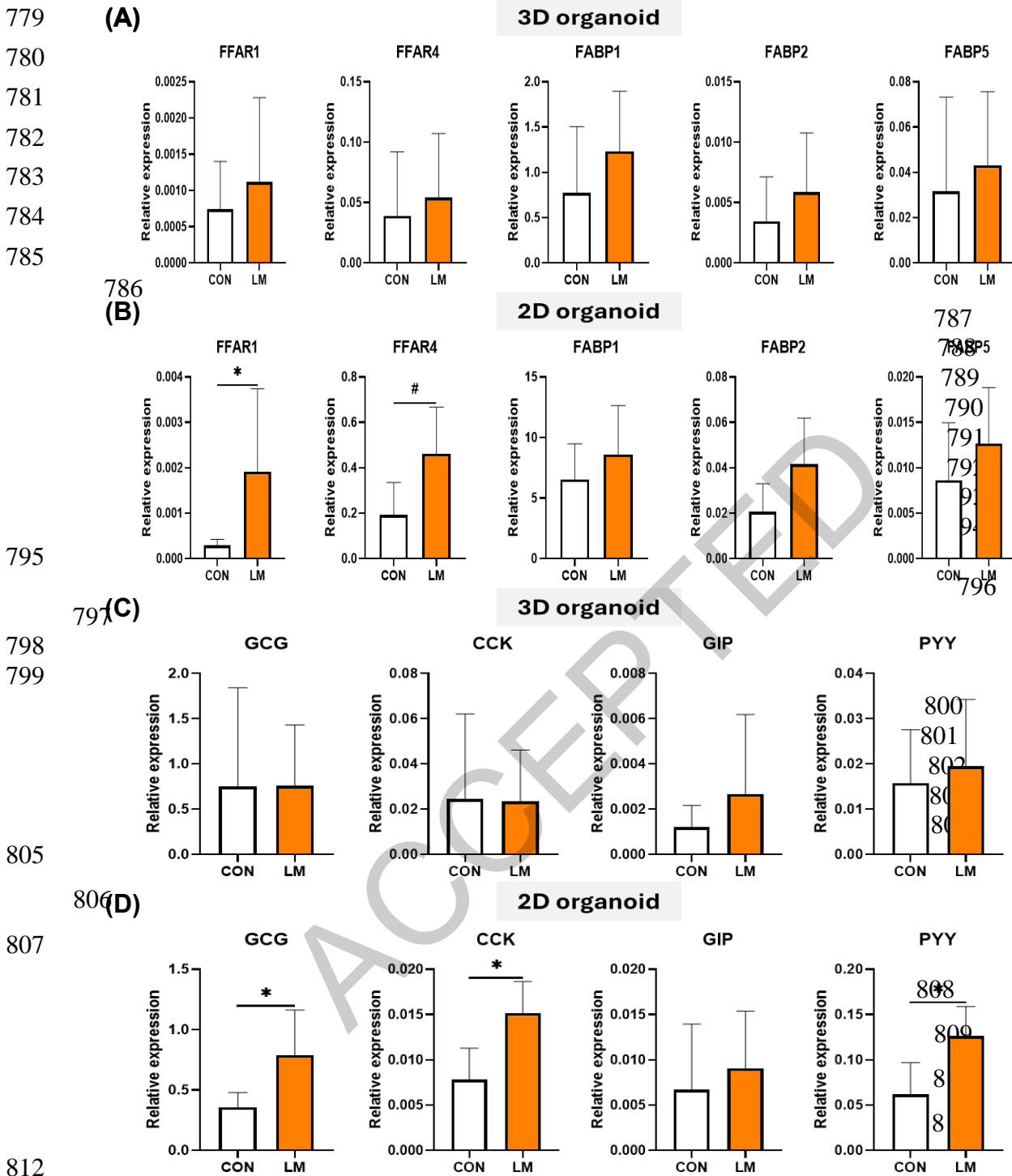


**Fig. 4 Fatty acid absorption of 3D and 2D pig intestinal organoids.** (A) Representative image of BODIPY-treated 3D and 2D pig intestinal organoids. Nucleus were stained with Hoechst 33342. Scale bar = 50  $\mu\text{m}$ . (B) Quantification of fatty acid analog absorption and fluorescent intensity in 3D and 2D pig intestinal organoids. Data are presented as mean  $\pm$  standard deviation (3D organoids n = 61, average 4.6 fluorescence area/organoid; 2D organoids n = 145, average 9.6 fluorescence area/image). \*\*\*  $p < 0.001$ .



813 **Fig. 5 Different fatty acid-related physiological responses of 3D and 2D pig intestinal organoids.** (A) Expression  
 814 of the mRNA levels of fatty acid receptor and fatty acid binding protein genes in 3D pig intestinal organoids. (B)  
 815 Expression of the mRNA levels of fatty acid receptor and binding protein genes in 2D pig intestinal organoids. (C)  
 816 Expression of the mRNA levels of hormone genes in 3D pig intestinal organoids. (D) Expression of the mRNA levels  
 817 of hormone genes in 2D pig intestinal organoids. Data are presented as mean  $\pm$  standard deviation ( $n = 3-5$ ).  $0.05 < \#p$   
 818  $< 0.10$ ;  $*p < 0.05$ .



820  
821  
822  
823  
824  
825  
826  
827  
828  
829  
830  
831  
832  
833  
834  
835  
836  
837  
838  
839  
840  
841  
842  
843  
844  
845  
846  
847  
848  
849  
850  
851  
852  
853  
854  
855  
856  
857  
858  
859  
860  
861

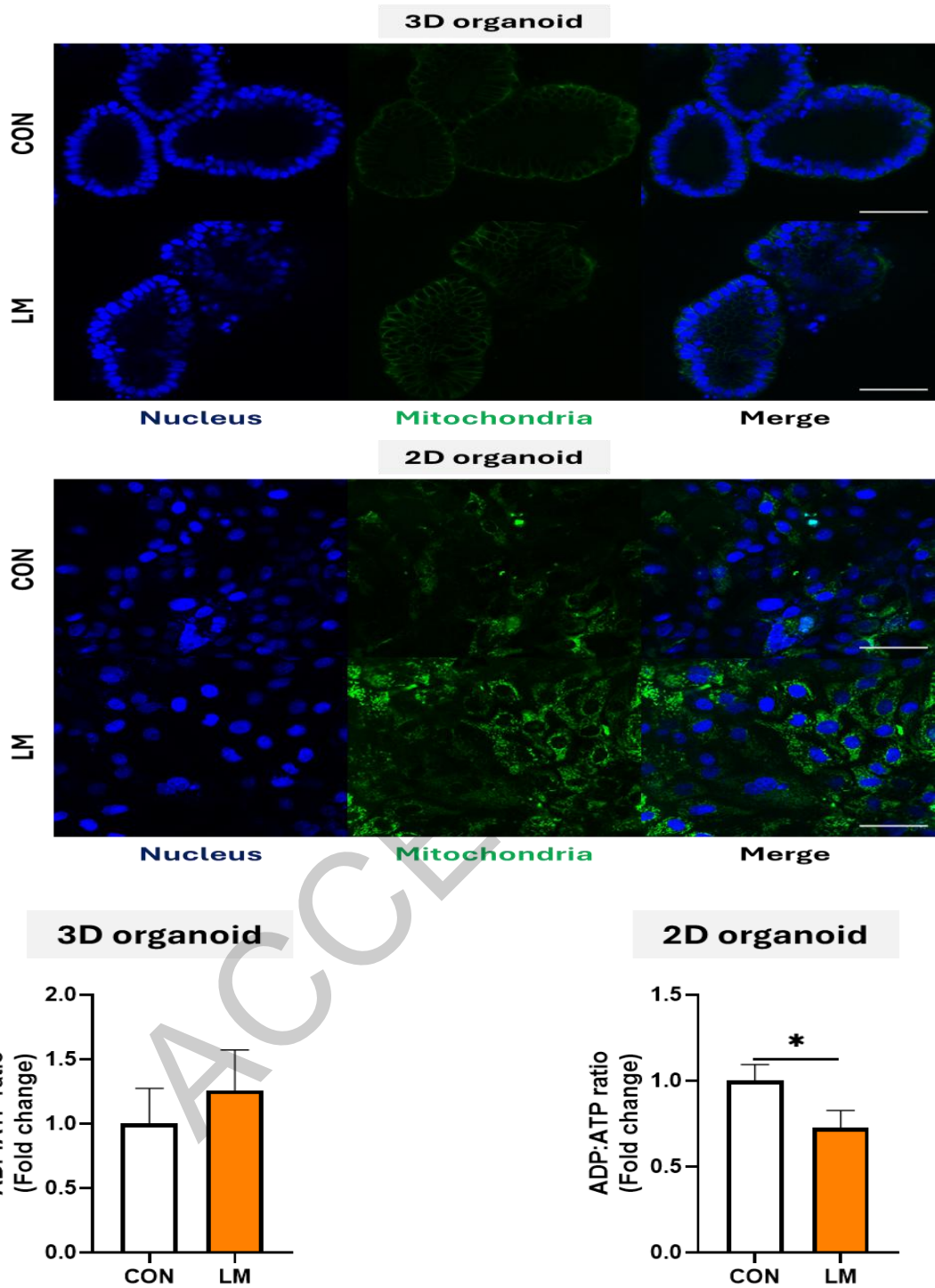


**Fig. 6 Fatty acid metabolic responses in 3D and 2D pig intestinal organoids.** (A) Representative mitochondria staining image of fatty acid-treated 3D and 2D pig intestinal organoids. Nucleus and mitochondria were stained with Hoechst 33342 and Mitotracker green FM. Scale bar = 50  $\mu$ m. (B) Relative mitochondrial ADP:ATP ratio of fatty acid-treated 3D and 2D pig intestinal organoids. Data are presented as mean  $\pm$  standard deviation (n = 3). \*  $p$  < 0.05.